



Novel anti-invasive properties of a Fascin1 inhibitor on colorectal cancer cells

Silvia Montoro-García¹ · Begoña Alburquerque-González² · Ángel Bernabé-García³ · Manuel Bernabé-García⁴ · Priscila Campioni Rodrigues^{5,6} · Helena den-Haan⁷ · Irene Luque⁸ · Francisco José Nicolás³ · Horacio Pérez-Sánchez⁹ · María Luisa Cayuela⁴ · Tuula Salo^{5,6,10,11} · Pablo Conesa-Zamora^{2,12}

Received: 22 January 2019 / Revised: 5 December 2019 / Accepted: 15 January 2020

© Springer-Verlag GmbH Germany, part of Springer Nature 2020

Abstract

Tumor invasion and metastasis involve processes in which actin cytoskeleton rearrangement induced by Fascin1 plays a crucial role. Indeed, Fascin1 has been found overexpressed in tumors with worse prognosis. Migrastatin and its analogues target Fascin1 and inhibit its activity. However, there is need for novel and smaller Fascin1 inhibitors. The aim of this study was to assess the effect of compound G2 in colorectal cancer cell lines and compare it to migrastatin in *in vitro* and *in vivo* assays. Molecular modeling, actin-bundling, cell viability, immunofluorescence, migration, and invasion assays were carried out in order to test anti-migratory and anti-invasive properties of compound G2. In addition, the *in vivo* effect of compound G2 was evaluated in a zebrafish model of invasion. HCT-116 cells exhibited the highest Fascin1 expression from eight tested colorectal cancer cell lines. Compound G2 showed important inhibitory effects on actin bundling, filopodia formation, migration, and invasion in different cell lines. Moreover, compound G2 treatment resulted in significant reduction of invasion of DLD-1 overexpressing Fascin1 and HCT-116 in zebrafish larvae xenografts; this effect being less evident in Fascin1 known-down HCT-116 cells. This study proves, for the first time, the *in vitro* and *in vivo* anti-tumoral activity of compound G2 on colorectal cancer cells and guides to design improved compound G2-based Fascin1 inhibitors.

Key messages

- Fascin is crucial for tumor invasion and metastasis and is overexpressed in bad prognostic tumors.
- Several adverse tumors overexpress Fascin1 and lack targeted therapy.
- Anti-fascin G2 is for the first time evaluated in colorectal carcinoma and compared with migrastatin.
- Filopodia formation, migration activity, and invasion *in vitro* and *in vivo* assays were performed.
- G2 blocks actin structures, migration, and invasion of colorectal cancer cells as fascin-dependent.

Keywords Fascin1 · Migrastatin · Invasion · Migration · Zebrafish xenograft · Colorectal cancer

Silvia Montoro-García and Begoña Alburquerque-González contributed equally to this work.

Electronic supplementary material The online version of this article (<https://doi.org/10.1007/s00109-020-01877-z>) contains supplementary material, which is available to authorized users.

✉ Silvia Montoro-García
smontoro@ucam.edu

✉ Pablo Conesa-Zamora
pablo.conesa@carm.es

Priscila Campioni Rodrigues
Priscila.CampioniRodrigues@oulu.fi

Extended author information available on the last page of the article

Introduction

Tumor metastasis remains the leading cause of cancer mortality [1]. Acquisition of invading capacity is a prerequisite for carcinoma cells to get access to vessels and thus spread throughout the body. This process involves actin cytoskeleton rearrangement allowing the tumor cells to develop cellular protrusions, such as filopodia and lamellipodium, which contribute to cancer cell migration, invasion, and metastasis [2]. Fascin1 (FSCN1: ENSG00000075618) is a key protein in membrane protrusion, as it possesses actin-binding and actin-bundling activity by cross-linking filamentous actin into tightly packed parallel bundles. Fascin1 expression is often elevated in malignant tumors

while its expression is low or absent in most normal adult epithelia [3]. Fascin1 has emerged as an important biomarker and therapeutic target due to its overexpression in several carcinomas and its association with mortality and metastasis [3, 4]. In fact, several studies including a meta-analysis have demonstrated that Fascin1 expression is associated with increased lymph node- and distant-metastasis, disease progression, and mortality in both colorectal and breast cancer [5, 6].

In a recent study, our group identified Fascin1 as overexpressed in serrated adenocarcinoma (SAC) [7], a histological subtype of colorectal carcinoma. SAC, in contrast to conventional colorectal carcinoma [8], has worse prognosis [9] and it is characterized by a more active invasive front evidenced by higher occurrence of tumor budding, cytoplasmic pseudofragments, infiltrative tumor growth pattern [10], and E-cadherin loss. Moreover, SACs show a higher frequency of KRAS and BRAF mutations than conventional carcinoma which make most of them resistant to anti-EGFR therapy [11, 12].

Given the causative role of Fascin1 in the invading phenotype of tumor cells together with the association of its overexpression to worse survival of a wide variety of cancer types [13–18], it would be desirable to find efficient Fascin1-activity blockers. In this line, migrastatin and its macroketone analogues are considered typical Fascin1 inhibitors [1]. Unfortunately, they are difficult to synthesize due to their complex structure [19].

In this study, we performed a search of patented potential Fascin1 inhibitors, such as those derived from indazol-furan-carboxamides [20]. Among them, we found the leading compound G2 and showed an inhibitory effect on Fascin1 activity by using several *in vitro* and *in vivo* assays on well-characterized colorectal cell lines.

Material and methods

Compounds and molecular modeling

Compound G2 (N-(1-(4-(trifluoromethyl) benzyl)-1H-indazol-3-yl) furan-2-carboxamide; C₂₀H₁₅F₃N₃O₂; PM 386.13) is covered by the patents WO 2014/031732 A2 and WO 2015/127125A1 and was synthesized as previously described [20]. Migrastatin was synthesized by AnalytiCon Discovery (NP-006108) and provided by MolPort (Riga, Latvia). The geometry of compound G2 was built with Autodock Tools [21], where partial charges were assigned using Gasteiger model [22]. The structural model for Fascin1 was extracted from the crystal structure of protein data bank (PDB) with code 6B0T [23] and converted to PDBQT format using default parameters. Molecular docking calculations based on the Blind Docking (BD) technique [24] were carried out using Blind Docking server (BDS, available at <http://bio-hpc.ucam.edu/achilles>) with Autodock 4 [21] as docking engine with default parameters. Graphical

representations of the docking results as PyMOL (<http://www.pymol.org>) sessions were downloaded from BDS with default options as specified on the website.

All the protocols comply with the recommendation, the approval of which was obtained from the participant institutions and in accordance with the ethical standards laid down in the 1964 Declaration of Helsinki and its later amendments.

Cell culture

Distinct human colorectal adenocarcinoma cell lines HCT-116, DLD-1, SW480, HCT-15, HT-29, LS174T, SW620, and LoVo were obtained from the American Type Culture Collection (ATCC, Rockville, MD, USA). Cell lines were cultivated using standard high glucose Dulbecco's Modified Eagle's Medium (DMEM) supplemented with 10% heat-inactivated fetal bovine serum (FBS), 50 U/mL penicillin, and 50 µg/mL streptomycin (all from Sigma-Aldrich Chemical Co., USA) at 37 °C and 5% CO₂ and 95% humidified atmosphere. Subculturing was performed when cells reached 90% confluence. Cell RNA extraction and qPCR for Fascin1 expression quantification is described in Supplementary Material S1. The human colorectal carcinoma cells were genetically overexpressed (DLD-1) and knocked-down (HCT-116) for Fascin-1 (Supplementary Material S1).

Cell viability assay

Exponentially growing cells were plated in flat-bottomed 96-well plates (Nunc, Roskilde, Denmark) in triplicate (1500 cells/well). Cells were treated with a series of concentrations from 500 nM to 100 µM of either migrastatin or compound G2 up to 3 days (24, 48, and 72 h) in a 5% CO₂-humidified atmosphere. Control cells were treated with drug carrier (0.1% dimethyl sulfoxide (DMSO)). Cells were assayed for viability as follows. Briefly, Dulbecco's phosphate-buffered saline (DPBS) supplemented with 1.9 mg/mL tetrazolium (MTT) pH 7.2 was added to the cells (30 µL/well). After incubation at 37 °C for 4 h, the medium was carefully aspirated. The formazan crystals were dissolved in 200 µL DMSO for 30 min and the absorbance was read in a microtiter plate reader at 570 nm and 620 nm as reference. Results were calculated as cell viability (%) = average optical density (O.D.) of wells/average O.D. of control wells.

Cell migration assay

Cell migration was studied using HCT-116 and DLD-1 cell lines by performing a scratch wound healing assay in standard medium supplemented with 5% FBS. Typically, 50,000 cells were plated in low 35-mm-dishes with culture inserts following manufacturer instructions (Ibidi, Martinsried, Germany). After appropriate cell attachment and monolayer formation

(around 24 h), inserts were removed with sterile forceps to create a wound field of approximately 500 μm . Detached cells were gently removed with DPBS before the addition of drugs. Confluent cells were incubated in one of the following treatments: control (0.1% DMSO), 100 μM migrastatin, 5, 10, and 20 μM compound G2. Cells were then placed in a cell culture incubator and they were allowed to migrate. At 0, 4, and 7 h (linear growth phase), 10 fields of the injury area were photographed with an inverted phase contrast microscope using $\times 10$ magnification. For each time point, the area uncovered by cells was determined by Image J software (National Institute of Health, Bethesda, MD, USA). Each treatment was performed in triplicate.

The migration speed of the wound closure was given as the percentage of the recovered area at each time point, relative to the initially covered area (t_0). The velocity of wound closure (%/h) was calculated according to the formula:

$$\text{Slope (\%/h)} = \frac{(\% \text{covered area } t_x) - (\% \text{covered area } t_o)}{(t_x - t_o)}$$

Slopes are expressed as percentages relative to control conditions.

Transwell invasion assay

The invasive capacity of HCT-116 cells was determined using Cytoselect TM 24 Well Cell Invasion Assay (Basement Membrane Colorimetric Format) with Matrigel^R-coated Transwell chambers (8 μm pore size) (Cell Biolabs Inc., CA, USA). Briefly, cells (9.5×10^4) were resuspended in serum-free medium with corresponding inhibitors (100 μM migrastatin and 20 μM compound G2) and seeded into the upper chamber. Additionally, 500 μL of standard medium were added to the well. After 30 h of incubation, cells that remained on the upper chamber were scraped away with a cotton swab, and the cells that had migrated through the matrigel and reached the bottom of the chamber were stained with the cell stain solution provided in the kit. Invasiveness was quantified by counting cells on the lower surface of the filter using Image J software (National Institute of Health, Bethesda, MD, USA). In addition, invasive cells at the bottom side of the filter were eluted and quantified at an absorbance of 560 nm.

Myoma organotypic invasion model

Tumoral cell invasion was assessed in the myoma organotypic cultures and performed according to the previously published myoma model protocol [25, 26]. Briefly, uterine leiomyoma tissues were obtained from routine surgery after informed consent of the donors and their use approved by The Ethics Committee of the Oulu University Hospital. The myoma tissue was sliced into 5 mm and disks were made with an 8-mm

biopsy punch (Kai Industries Co., Gifu, Japan). Myoma disks were preincubated in either 0.1% DMSO, 100 μM migrastatin or 10 μM and 20 μM compound G2 at 4 $^\circ\text{C}$ for 48 h. The myoma disks were placed into Transwell inserts (diameter 6.5 mm; Corning Incorporated, Corning, NY) and 700,000 cells in 50 μL of media were added on top of each myoma disk. Cells were allowed to attach overnight and the myoma disks, transferred onto uncoated nylon disks and be treated with the compounds for 14 days, while changing the treatment media every 3 days. Subsequently, the myoma discs were fixed with 4% neutral-buffered formalin for 24 h and 6 μm sections were cut and stained with cytokeratin AE1/AE3 (M3515, Dako). Sections were documented at $\times 10$ magnifications, using the Leica DMRB microscope DFC 480 camera with the Leica application suite v3.8 (Leica Microsystems, Wetzlar, Germany). Image J software (National Institute of Health, Bethesda, MD, USA) was used to measure invasion areas and depths. Each treatment was performed in triplicate.

Zebrafish invasion assays and treatments

The colonization of zebrafish (ZF) (*Danio rerio*) embryos by human cancer colorectal cell lines was performed as previously described [27]. The experiments performed comply with the Guidelines of the European Union Council (Directive 2010/63/EU) and the Spanish RD 53/2013. Experiments and procedures were performed as approved by the Bioethical Committee of the Murcia University (Spain). Briefly, human cell lines were trypsinized, washed, and stained with fluorescent CM-Dil (Vibrant, Invitrogen) following manufacturer's instructions. Fifty to 100 labeled cells were injected into the yolk sac of dechorionated ZF embryos and transferred into 24-well plates. Fish with fluorescently labeled cells appearing outside the implantation area at 2 h post-injection (dpi) were excluded from further analysis. All other fishes were treated, by bath immersion, with E3 medium (5 mM NaCl, 0.33 mM KCl, 0.33 mM CaCl₂, 0.33 mM MgSO₄, 0.1% methylene blue) (all from Sigma-Aldrich, St Louis, MO, USA) supplemented with either 100 μM migrastatin or 5–10 μM compound G2 for 96 h at 35 $^\circ\text{C}$. Treatment was renewed every 24 h. Larvae analyzed with a M205-FA stereomicroscope equipped with a DFC365FX camera (Leica). The evaluation criteria for embryos being colonized by human cancer cells was the presence of more than three cells outside of the yolk sac and, with this criterion, ZF percentage of invasion was calculated.

With the aim of finding out whether the pro-metastatic activity of Fascin1-induced expression was affected by chemical compounds, a metastasis assay was carried out. Zebrafish embryos xenografted with Fascin1-transfected DLD-1 cells were incubated up to 144 h. The day of invasion screening (fourth day post-xenograft), freshly prepared E3 medium was supplemented with 100 μM migrastatin or 10 μM compound G2 together with 375 rotifers/mL (*Brachionus plicatilis* (L-

type); ReefNutrition, Campbell, CA, USA). The number of small colonies generated from individual invading cells was counted on the sixth day post-xenograft (6 dpi). This was considered as the number of ZF larvae with metastasis.

Data analysis

Data are expressed as mean \pm standard deviation (SD). Data were analyzed for statistical differences by the Student's *t* test for paired and unpaired data after testing for normal distribution of the data. For in vitro experiments, one-way analysis of variance (ANOVA) was performed followed by a Tukey post hoc test to compare each group. Differences were considered significant at an error probability of $p < 0.05$. SPSS 18.0 software was used for the rest of statistical analyses (SPSS, Inc., Chicago, IL, USA). For myoma assay, OriginPro 2016 software was used for statistical calculations. One-way ANOVA (analysis of variance) with post hoc comparisons based on the Tukey's multiple comparisons test were applied. The level of significance considered was 5% ($p \leq 0.05$).

Results

Molecular modeling

Figure 1 shows the main resulting pose of compound G2 after blind docking calculations against whole Fascin1 protein

surface. Most relevant intermolecular interactions established are related to hydrogen bonds (GLU215), pi-pi (TRP101), and hydrophobic interactions (LEU16, PHE14, LEU48, ILE93, VAL134, GLU215, PHE216). It must be noticed that these residues participate in the actin-binding site 2, located within the pocket formed by β -trefoil 1 and 2 from the Fascin1 structure, and that blind docking calculations were able to predict this interaction spot with no previous assumption about binding site. In addition, this prediction coincides rather well with crystallographic pose of ligand compound G2-029 (PDB: 6B0T), which is to be expected due to the small difference between compound G2 and G2-029 molecules, just a methyl group.

Compound G2 prevents in vitro Fascin1-induced F-actin bundling

In order to assess the effect of compound G2 on Fascin1, we performed an F-actin-bundling assay under transmission electron microscopy (TEM) (Supplementary Material S1). As shown in Fig. 2, only F-actin incubated in the presence of untreated Fascin1 formed filament bundles (12.00 [9.00–19.75]). Fascin1 preincubated with 100 μ M migrastatin or compound G2 (up to 20 μ M) lead to the disorganization of the bundles, resulting in fewer filaments than in control conditions (Kruskal-Wallis test, $p < 0.001$). No statistically changes were found between the different drug treatments (Kruskal-Wallis test, $p = 0.370$).

Fig. 1 Main interactions obtained after blind docking of compound G2 against Fascin1. Blue solid line represents hydrogen bond, green dashed line aromatic interactions, and dashed gray lines hydrophobic interactions. Inset: compound G2 chemical structure

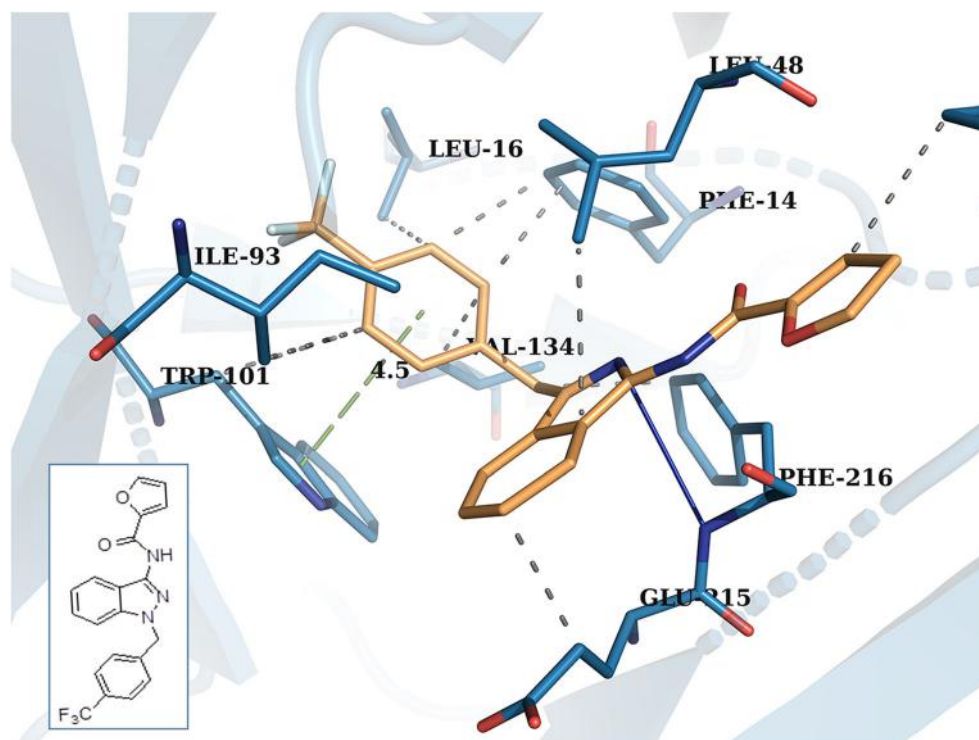
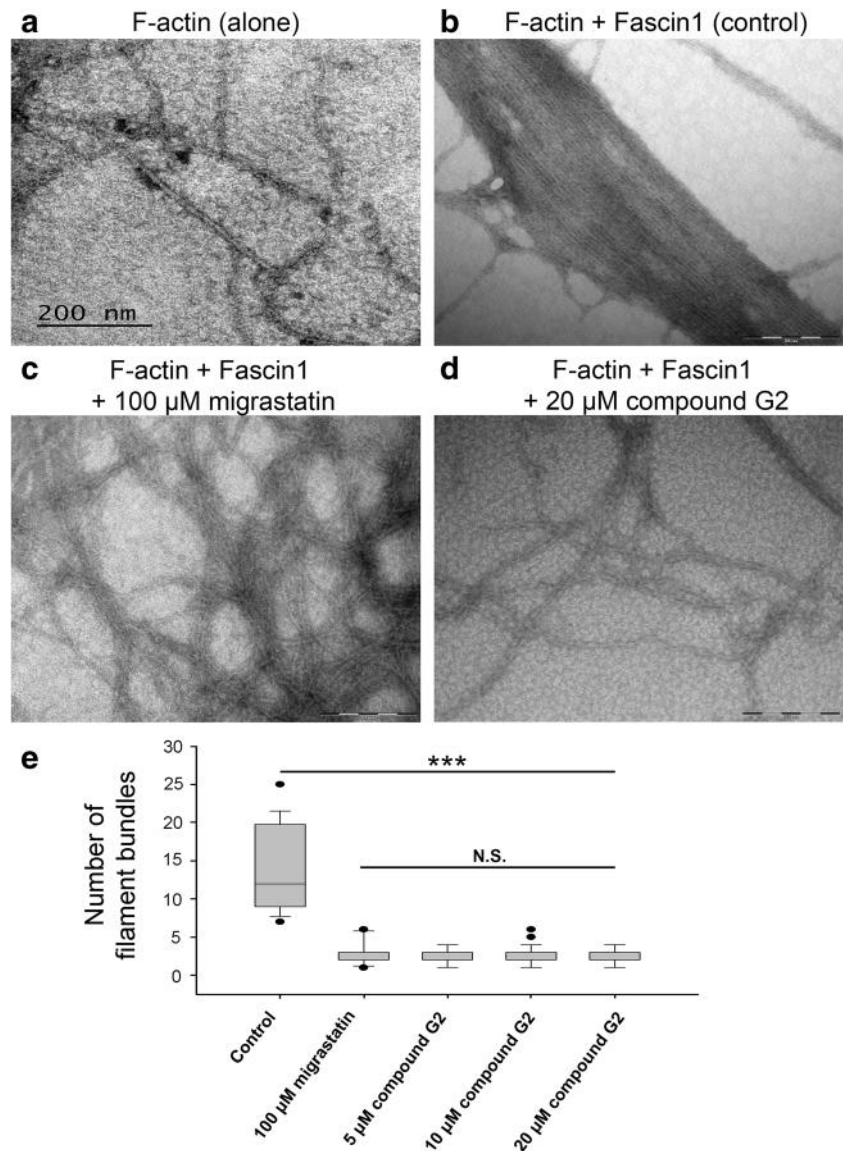


Fig. 2 Transmission electronic microscopy visualization of actin-binding and bundling activities of Fascin1 treated or not with inhibitors (negative staining). **a** Stained F-actin filaments alone. **b** F-actin-bundling assay with filamentous F-actin and untreated Fascin1 (1:1 molecular ratio) (control condition). **c** F-actin-bundling assay with filamentous F-actin and Fascin1 previously incubated with 100 μ M migrastatin (1:1 molecular ratio). **d** F-actin-bundling assay with filamentous F-actin and Fascin1 previously incubated with 20 μ M compound G2. Magnification: **a** \times 120,000 and **b** to **d** \times 93,000. **e** Quantitative analysis of the numbers of actin filaments bundles in the stated conditions (** p < 0.001 compared to control condition), non-significant (N.S.) between treatments (Kruskal-Wallis test)



Compound G2 affects cytoskeleton formation and Fascin1 localization at the lamellipodium

In order to choose colorectal cell lines with highest and lowest endogenous Fascin1 expression, a RT-qPCR was performed upon RNA extracted from eight cell lines. As shown in Supplementary Material 2, HCT-116 and SW480 exhibited the highest Fascin1 expression while LoVo, DLD-1, and HT-29 had the lowest. Given the ease for cell culture and the differences in endogenous Fascin1 expression, we selected DLD-1 (low Fascin1 expression) and HCT-116 (high Fascin1 expression) cell lines in subsequent assays.

To assess the Fascin1 inhibition activity of the compound G2 on cell viability, we tested different concentration of migrastatin and compound G2 on different colorectal cancer cells. As shown Supplementary Material S3, migrastatin was

generally better tolerated than compound G2 by the DLD-1 and HCT-116 cell lines. Thus, the working concentrations for migrastatin and compound G2 were set up for subsequent in vitro studies at 100 μ M and up to 20 μ M, respectively.

The effect of compound G2 on Fascin1 localization and the reorganization of the actin cytoskeleton as well as on the protrusion of lamellipodium at the cell front was assessed by immunofluorescence. For that purpose, we used HCT-116, the colorectal cell line with maximum expression levels of Fascin1 together with Fascin1 silenced HCT-116 cells. As shown in Fig. 3, prominent lamellipodium formation was observed in control conditions and for EGF-treated cells (non-significant differences between each other were found). However, these cytoskeleton structures were absent in cells treated with migrastatin and compound G2, similarly to what it was observed with PD98059, an inhibitor targeting the MEK pathway. Lamellipodium protrusion

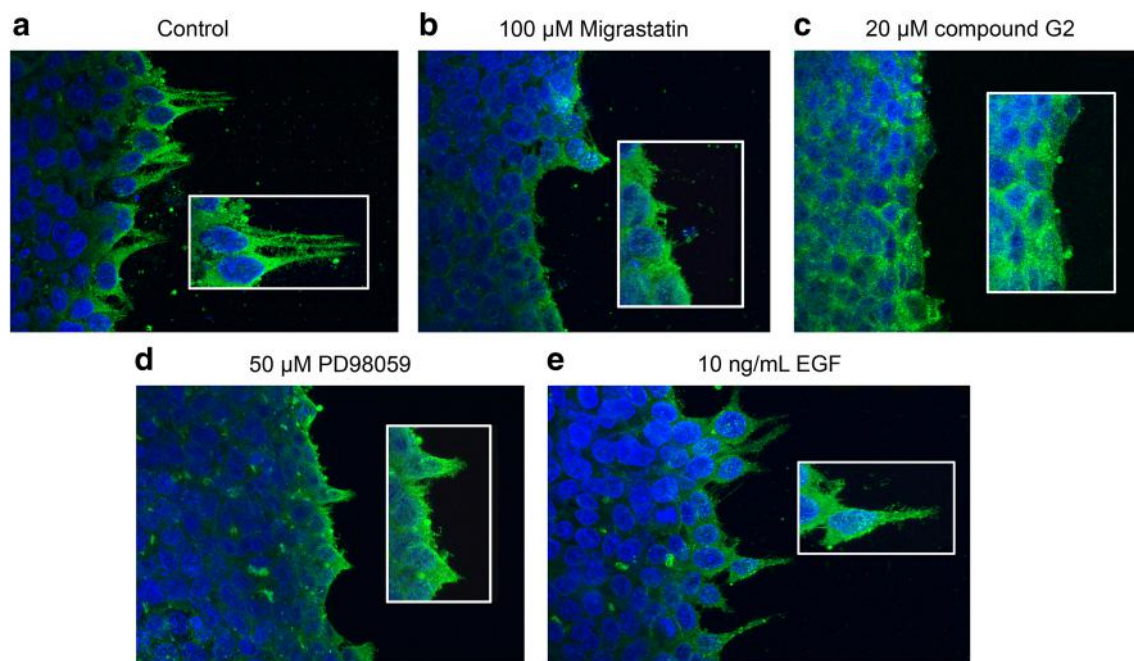


Fig. 3 Migrastatin and compound G2 affect lamellipodium formation and morphology of HCT-116. Representative images of immunofluorescence assays for Fascin1 (lower inset in detail) are shown. **a** Control condition; **b** 100 μ M migrastatin; **c** 20 μ M compound G2; **d** 50 μ M PD98059 (Mek inhibitor); **e** 10 ng/mL epidermal growth factor (EGF, migration stimulator). Cells were fixed

and stained with anti-Fascin1 antibody (1/250). Images were captured with a LSM 510 META confocal fluorescence microscope with $\times 63$ oil objective. Fascin1 location is shown in green in these structures. Co-staining with Hoechst-33258 was used to show the cell nuclei. Both migrastatin and compound G2 inhibited lamellipodium protrusion and Fascin1 localization in a similar way to the migration Mek inhibitor

numbers calculated at different conditions were significantly lower upon both migrastatin and compound G2 treatments when compared to control conditions (Table 1). Supplementary Material S4 showed that the treatments also abolished the actin bundles in lamellipodium. Similar results were observed with an extra cell line expressing Fascin1 (HaCat) as DLD1 morphology was not suitable for assessing lamellipodium formation (data not shown). Transcriptional Fascin1 silencing of HCT-116 abolished the Fascin1 accumulation at lamellipodium sites and produced an alteration of F-actin microfilament assembly in silenced cells (Supplemental S5D).

Compound G2 diminishes migration and inhibits Matrigel cell invasion of colorectal cancer cells

In order to correlate the observed effect of Fascin1 inhibitors on lamellipodium protrusion to an effect on cell migration, migrastatin- and compound G2-treated cells were investigated

for their migration activity using an in vitro wound healing scratch assay. As shown in Fig. 4, compound G2 produces a remarkable inhibition of migration in HCT-116 and DLD-1 cell lines ($p < 0.01$). Compound G2 effect at 20 μ M was more pronounced than migrastatin in DLD-1 cells, while in HCT-116 the effect of compound G2 on migration was lower.

Tumor cell invasion not only involves the acquisition of migration properties but also the ability to degrade the basement membrane and tumor stroma matrices, three-dimensional substrates [28]. For that reason, we performed a Transwell assay on Matrigel^R which resembles the basement membrane extracellular matrix composition. As shown in Supplementary Material S6, both compound G2 and migrastatin inhibit tumor cell invasion of HCT-116, the effect of the latter being slightly more evident.

To further confirm the inhibitory effect of compound G2 on the Fascin1 activity, we used Fascin1 silenced HCT116 and fascin1 overexpressed DLD-1 cells and

Table 1 Lamellipodium protrusion numbers in the different conditions in HCT-116 cells

	Control	100 μ M migrastatin	20 μ M compound G2	10 ng/mL EGF	50 μ M PD98059
Lamellipodium numbers	9 \pm 1.5	2 \pm 2	5.8 \pm 1.1	10.4 \pm 1.5	1 \pm 1
<i>p</i> value*		0.000139	0.002936	0.140178	5.9241E ⁻⁰⁶

*Student *T* test compared to control condition

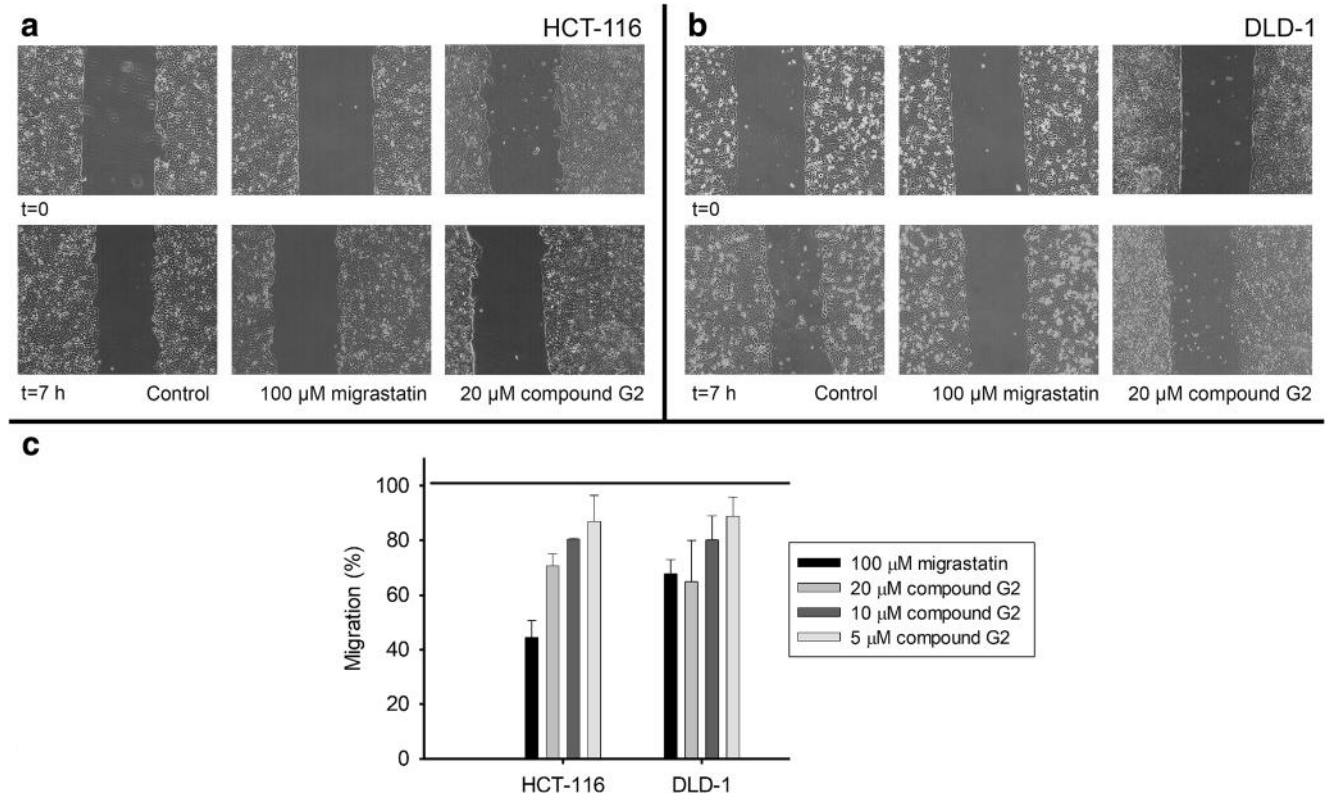


Fig. 4 Migrastatin and compound G2 prevent cell migration on HCT-116 and DLD-1 colorectal cancer cells. **a** Effect of 100 μM migrastatin and 20 μM compound G2 on HCT-116 and **b** DLD-1 cells. **c** Percentage of migration for 100 μM migrastatin and compound G2 (5, 10, 20 μM)

treatments. Migration was calculated with respect to the control conditions (100%) for a slope between 4 and 7 h (lineal phase). ** $p < 0.01$

tested their migration and invasion properties. Fascin1 silencing produces a slight decrease of migration and invasion compared to MOCK HCT-116 cells ($p < 0.05$), whereas double inhibition (genetic and pharmacological) only produced a significant decrease in migration (Supplemental material S7A-B). Accordingly, 10 μM compound G2 strongly diminished migration and invasion in Fascin1 overexpressed DLD-1 cells ($p < 0.01$) (Supplemental material S7C-D).

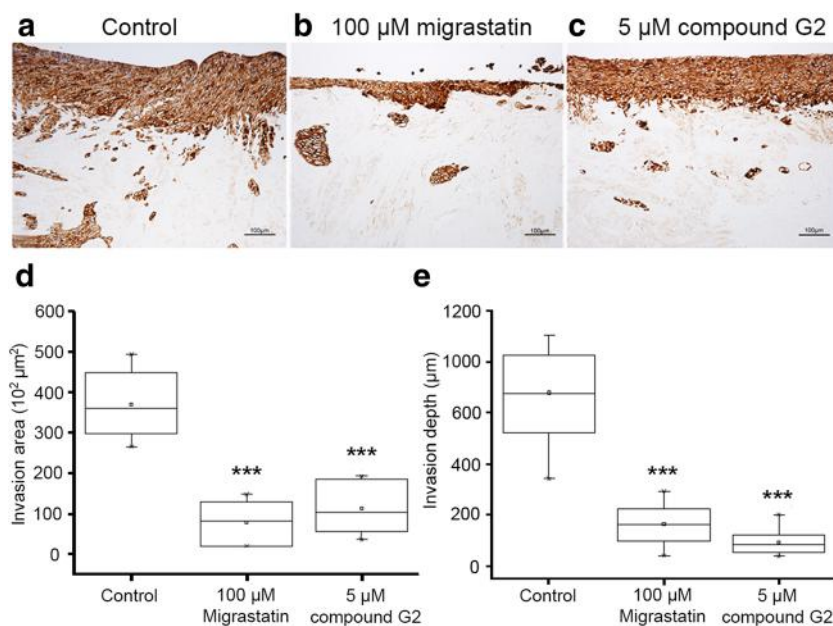
Compound G2 diminishes HCT-116 colon cancer cell invasion in a human benign leiomyoma tissue in vitro 3D model

In order to find out whether the anti-invasive properties of compound G2 on cancer cell invasion could be translated into a 3D human model, a myoma disc organotypic model was used. As shown in Fig. 5, compound G2 (5 μM) significantly reduced the invasion depth and invasion area of HCT-116 cells into the discs when compared to untreated cells ($p < 0.01$). Similar results were obtained when cells were treated with 10 and 20 μM compound G2 (Supplementary Material S8).

Compound G2 inhibits the invasive capacity of HCT-116 tumor cells in an in vivo assay of zebrafish model

In order to find out whether the anti-invasive properties of compound G2 could be extrapolated to a living animal, a xenograft assay was carried by using the well-established zebrafish (ZF)-larvae invasion model. To test viability, groups of thirty larvae were treated with either 100 μM migrastatin or 5, 10, and 20 μM compound G2. The majority of larvae were viable after 30 days treatment with either 5 or 10 μM . However, 20 μM compound G2 treatment caused larvae death at the third day of treatment (Supplementary Material S9A). Therefore, concentrations chosen for ZF assays were 5 and 10 μM compound G2. Later on, detached and labeled colorectal cancer cells were injected into the yolk sac and colonization was followed up to 6 days. The percentage of invasion was studied for four colorectal cancer cell lines (Fig. 6a, b) that exhibited different Fascin1 expression levels (Supplementary Material S2). HCT-116 and DLD-1 were selected for being the cell lines with the highest and lower Fascin1 expression, respectively. Good correlation was observed between Fascin1 expression and cell invasion for all cell lines assayed except HCT-15 whose invasion was lower than expected (Fig. 6b) possibly due to other fascin1 independent factors

Fig. 5 Myoma organotypic invasion model in HCT-116 cell line. **a** Invasion of the cells within myoma discs after treatment in control conditions, **b** 100 μ M migrastatin, and **c** 5 μ M compound G2. Pictures were taken under a phase contrast microscope with $\times 100$ magnification and 100 μ m scale bars. **d** The invasion area and **e** invasion depth of cytokeratin positive cells were quantified with image J. Data is shown as mean \pm SD compared with the control. *** $p < 0.001$



affecting invasion [29]. Therefore, and because of good correlation, HCT-116 was selected for being the cell line with the highest and DLD-1 for its lower Fascin1 expression and cell invasion. To further test the *in vivo* involvement of Fascin1 in this phenomenon, we performed exogenous silencing of Fascin1 in HCT-116 cells (Fig. 7a). Either genetic reduction of Fascin1 or its pharmacological inhibition by compound G2 decreased the invasion in HCT-116 cells (Fig. 7b, c). Conversely, we induced the overexpression of Fascin1 by means of plasmid transfection into DLD-1 cells (Fig. 7d), thus correlating with a higher invasion capacity (Fig. 7e). Compound G2 kept inhibiting invasion in both MOCK and transfected Fascin1-overexpressing cells (Fig. 7f). Consequently, *in vivo* invasion correlated with Fascin1 expression and compound G2 inhibited it in transfected

cells (Fig. 7e, f). Furthermore, a clear increase of the number of ZF larvae with metastasis was observed with Fascin1-overexpressing DLD-1 cells although 10 μ M compound G2 treatment had a similar effect on ZF groups subjected to either Fascin1 transfected or wild-type DLD-1 cells (Supplementary Material S10).

Discussion

Colorectal serrated adenocarcinoma and triple negative breast carcinoma are characterized by their bad prognosis, overexpression of Fascin1, and the absence of targeted molecular therapy [7, 8, 12, 30–35]. Han et al. demonstrated an

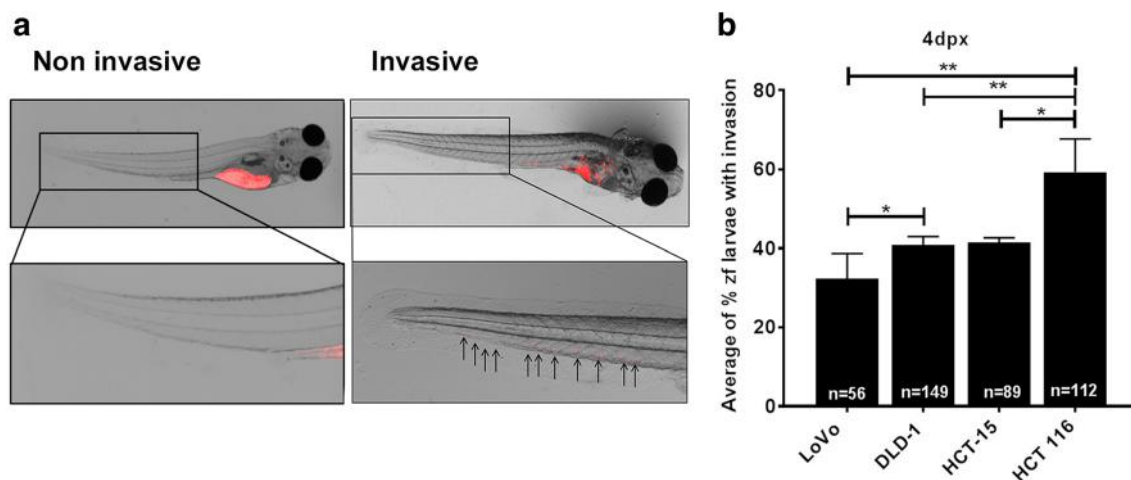


Fig. 6 Zebrafish invasion assays. **a** Zebrafish invasion model. Representative images of a zebrafish embryo with no invasion where the labeled cells remained in the yolk and never invaded the embryo and an embryo with invasion where the cells were able to migrate

outside of the yolk. Magnification of the tail region of an embryo with invasion is shown at the right. **b** Invasiveness of each cell line in this model. Data is shown as mean \pm SD; compared with the control. * $p = 0.049$ – 0.01 ; ** $p = 0.001$ – 0.009

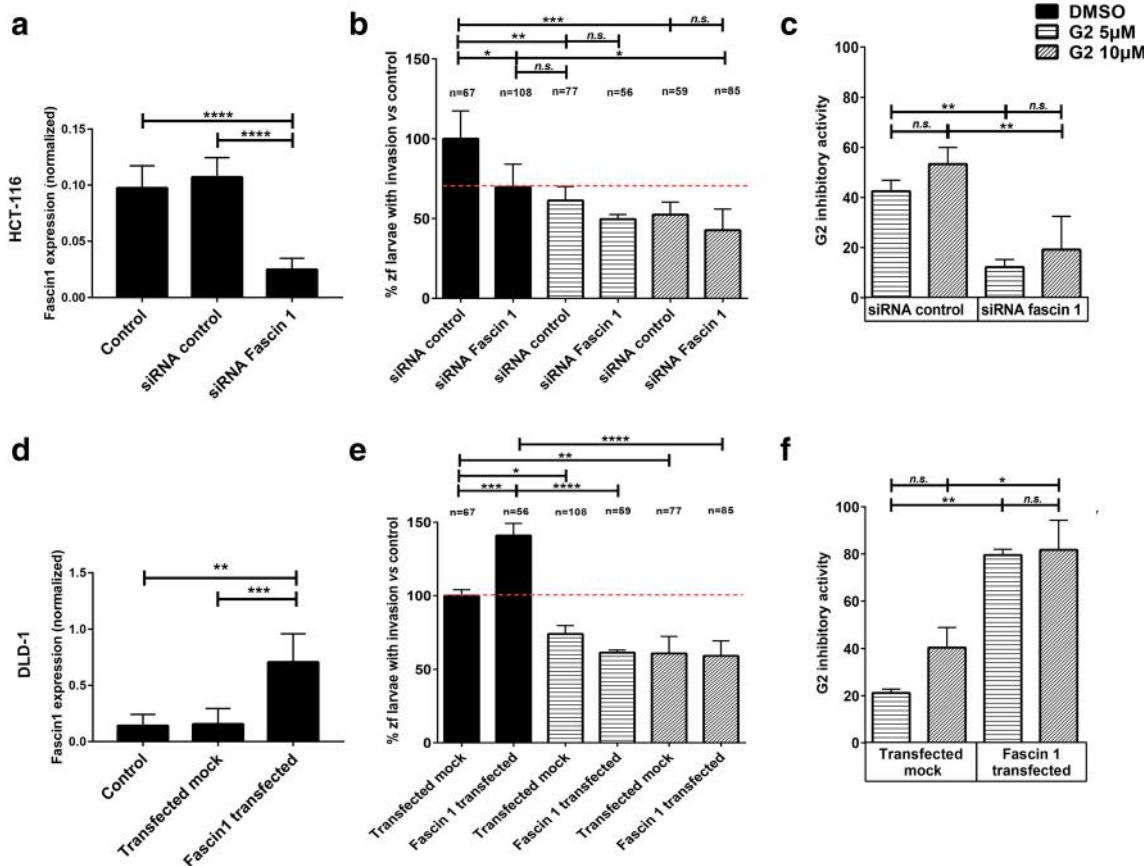


Fig. 7 Treatment effects on cancer cell invasion with different grades of Fascin1 expression. **a** Inhibition of Fascin1 gene expression upon siRNA-Fascin1 transfection in HCT-116 cells. **b** Effect of 5 and 10 μ M compound G2 on HCT-116 invasion with endogenous and silenced Fascin1 expression. **c** Compound G2 inhibitory activity on control and siRNA Fascin1-transfected HCT-116 cells. First two columns represent the difference between percentage of invasion in control (MOCK) and percentage of invasion in treated cells. Second two columns represent the difference between percentage of invasion in siRNA Fascin1-transfected HCT-116 and percentage of invasion in compound G2-treated siRNA Fascin1-transfected HCT-116 cells. Note that the effect of compound G2 decreased when Fascin1 was silenced. **d** Overexpression of Fascin1

gene upon Fascin1 transfection in DLD-1. **e** Effect of 5 and 10 μ M compound G2 on DLD-1 invasion with endogenous and exogenous Fascin1 expression. **f** Compound G2 inhibitory activity on control and Fascin1-transfected DLD-1 cells. First two columns represent the difference between percentage of invasion in control (MOCK) and percentage of invasion in treated cells. Second two columns represent the difference between percentage of invasion in Fascin1-transfected DLD-1 and percentage of invasion in compound G2-treated Fascin1-transfected DLD-1. Note that the effect of compound G2 increased when Fascin1 was overexpressed by transfection. Data is shown as mean \pm SD; compared with the control, * p = 0.049–0.01. ** p = 0.001–0.009. *** p = 0.0001–0.0009. **** p < 0.0001

inhibitory effect of compound G2 and its derivatives on Fascin1-driven actin bundling. Moreover, they showed an anti-migratory and anti-invasive effect of compound G2 on breast cancer cells [20]. In the present report, we include a molecular model, which provided an improved understanding regarding atomic details of the interactions between compound G2 chemical class and Fascin1 inhibition and will guide the future identification of more potent anti-metastatic drugs. Using blind docking calculations, the model identified a region in Fascin1 possibly involved in compound G2 binding. Some prior evidences support this finding as this region is part of the actin-binding site 1, as described by Han et al. [20]. In accordance, preincubation of Fascin1 with migrastatin and compound G2 disrupted the F-actin bundle formation in vitro. Herein, among the different colorectal cell lines used in this study, HCT-116 expressed the highest Fascin1 levels and its

migration capacity was clearly reduced after treatment with compound G2, even at lower concentrations than migrastatin and in a dose-dependent manner. Invasion and confocal studies were further performed with HCT-116 cells because of its morphological features and higher Fascin1 expression levels. We showed that both inhibitors, migrastatin and compound G2, strongly abolished the protrusion of lamellipodium, as confirmed by rescue experiments in Fascin1-silenced cells. Furthermore, we observed similar inhibitory effects of migrastatin and compound G2 on the Matrigel invasion assays with naïve and transfected HCT-116 and DLD-1 cells. Myoma discs represent a superior 3D model for cancer cell invasion studies compared to the other, non-human tissue-based, organotypic models [36]. In myoma assay, both migrastatin and compound G2 were similarly able to significantly decrease both the invasion depth and invasion area of HCT-

116 cells. It is important to notice that cell death caused by long-time incubation with the compound G2 was avoided in the migration and invasion *in vitro* assays, since viability did not seem to be compromised after 30 h. Of note, no previous studies have analyzed the effect of migrastatin or compound G2 on human solid, hypoxic, myoma disc organotypic invasion assay.

Moreover, *in vivo* assays using a model of ZF where Fascin1 expression was modified in colorectal cells showed that compound G2 effects on colorectal cancer cells invasion capacities showed a Fascin1 dependency. This compound inhibits the invasion of two cell lines of colorectal cancer with high expression of Fascin1, both constitutive and induced, without affecting the ZF viability and with a more pronounced effect than migrastatin. This activity also had an effect on colony formation from individual invading cells thus suggesting an inhibition of both invasion and metastasis of Fascin1-transfected tumor cells. It is worth of mentioning that this validated model was capable of testing a very high number of individuals per assay. However and despite these evidences, additional off-target anti-tumoral effects of G2 apart from Fascin1 are also possible.

In conclusion, this study reports a Fascin1 inhibitor with anti-migratory and anti-invasive properties in colorectal cancer cells at lower concentrations than migrastatin, the typical Fascin1 inhibitor. Using this strategy, we have here confirmed a novel class of compounds for the study of therapeutic approaches for invasive and metastatic tumoral cells, such as SAC, providing the first rationale for a tailored therapy in this type of cancer.

Acknowledgments This research was partially supported by the e-infrastructure program of the Research Council of Norway, and the supercomputer center of UiT, the Arctic University of Norway, and by the supercomputing infrastructure of Poznan Supercomputing Center.

Funding information This project received grants from Instituto de Salud Carlos III (Spanish Ministry of Health) and FEDER funds (ref: PI12/1232 and PI15/00626), Spanish Ministry of Economy and Competitiveness MINECO (CTQ2017-87974-R), and by the Fundación Séneca del Centro de Coordinación de la Investigación de la Región de Murcia under Projects 18946/JLI/13 and 20646/JLI/18. BAG belongs to the “Programa de Doctorado en Ciencias de la Salud, Universidad Católica de Murcia (UCAM)” and holds a grant of the UCAM. PCR was supported by Finnish Cultural Foundation Grant (2017-2018).

Compliance with ethical standards

Conflict of interest The authors declare that there are no conflicts of interest.



References

- Chen L, Yang S, Jakoncic J, Zhang JJ, Huang XY (2010) Migrastatin analogues target fascin to block tumour metastasis. *Nature* 464(7291):1062–1066
- Machesky LM, Li A (2010) Fascin: Invasive filopodia promoting metastasis. *Commun Integr Biol* 3(3):263–270
- Hashimoto Y, Kim DJ, Adams JC (2011) The roles of fascin in health and disease. *J Pathol* 224(3):289–300
- Hashimoto Y, Skacel M, Adams JC (2005) Roles of fascin in human carcinoma motility and signaling: prospects for a novel biomarker? *Int J Biochem Cell Biol* 37(9):1787–1804
- Omran OM, Al Sheeha M (2015) Cytoskeletal focal adhesion proteins Fascin-1 and Paxillin are predictors of malignant progression and poor prognosis in human breast cancer. *J Environ Pathol Toxicol Oncol* 34(3):201–212
- Tan VY, Lewis SJ, Adams JC, Martin RM (2013) Association of fascin-1 with mortality, disease progression and metastasis in carcinomas: a systematic review and meta-analysis. *BMC Med* 11:52
- Conesa-Zamora P, García-Solano J, García-García F, Turpin Mdel C, Trujillo-Santos J, Torres-Moreno D, Pérez-Guillermo M (2013) Expression profiling shows differential molecular pathways and provides potential new diagnostic biomarkers for colorectal serrated adenocarcinoma. *Int J Cancer* 132(2):297–307
- García-Solano J, Conesa-Zamora P, Carbonell P, Trujillo-Santos J, Torres-Moreno DD, Pagán-Gómez I, Rodríguez-Braun E, Pérez-Guillermo M (2012a) Colorectal serrated adenocarcinoma shows a different profile of oncogene mutations, MSI status and DNA repair protein expression compared to conventional and sporadic MSI-H carcinomas. *Int J Cancer* 131(8):1790–1799
- García-Solano J, Pérez-Guillermo M, Conesa-Zamora P, Acosta-Ortega J, Trujillo-Santos J, Cerezuola-Fuentes F, Mäkinen MJ (2010) Clinicopathologic study of 85 colorectal serrated adenocarcinomas: further insights into the full recognition of a new subset of colorectal carcinoma. *Hum Pathol* 41(10):1359–1368
- García-Solano J, Conesa-Zamora P, Trujillo-Santos J, Mäkinen MJ, Pérez-Guillermo M (2011) Tumour budding and other prognostic pathological features at invasive margins in serrated colorectal adenocarcinoma: a comparative study with conventional carcinoma. *Histopathology* 59(6):1046–1056
- García-Solano J, Conesa-Zamora P, Trujillo-Santos J, Torres-Moreno D, Mäkinen MJ, Pérez-Guillermo M (2012b) Immunohistochemical expression profile of β -catenin, E-cadherin, P-cadherin, laminin-5 γ 2 chain, and SMAD4 in colorectal serrated adenocarcinoma. *Hum Pathol* 43(7):1094–1102
- Stefanius K, Ylitalo L, Tuomisto A, Kuivila R, Kantola T, Sirmö P, Karttunen TJ, Mäkinen MJ (2011) Frequent mutations of KRAS in addition to BRAF in colorectal serrated adenocarcinoma. *Histopathology* 58(5):679–692
- Cao HH, Zheng CP, Wang SH, Wu JY, Shen JH, Xu XE, Fu JH, Wu ZY, Li EM, Xu LY (2014) A molecular prognostic model predicts esophageal squamous cell carcinoma prognosis. *PLoS One* 9(8):e106007
- Jones RP, Bird NT, Smith RA, Palmer DH, Fenwick SW, Poston GJ, Malik HZ (2015) Prognostic molecular markers in resected extrahepatic biliary tract cancers; a systematic review and meta-analysis of immunohistochemically detected biomarkers. *Biomark Med* 9(8):763–775
- Li A, Morton JP, Ma Y, Karim SA, Zhou Y, Faller WJ, Woodham EF, Morris HT, Stevenson RP, Juin A et al (2014) Fascin is regulated by slug, promotes progression of pancreatic cancer in mice, and is associated with patient outcomes. *Gastroenterology* 146(5):1386–1396.e1381-1317
- Rodrigues PC, Sawazaki-Calone I, Ervolino de Oliveira C, Soares Macedo CC, Dourado MR, Cervigne NK, Miguel MC, Ferreira do Carmo A, Lambert DW, Graner E (2017) Fascin promotes migration and invasion and is a prognostic marker for oral squamous cell carcinoma. *Oncotarget* 8(43):74736–74754
- Stewart CJ, Crook ML (2015) Fascin expression in undifferentiated and dedifferentiated endometrial carcinoma. *Hum Pathol* 46(10):1514–1520

18. Zhao W, Gao J, Wu J, Liu QH, Wang ZG, Li HL, Xing LH (2015) Expression of Fascin-1 on human lung cancer and paracarcinoma tissue and its relation to clinicopathological characteristics in patients with lung cancer. *Onco Targets Ther* 8:2571–2576
19. Gaul C, Njardarson JT, Shan D, Dorn DC, Wu KD, Tong WP, Huang XY, Moore MA, Danishefsky SJ (2004) The migrastatin family: discovery of potent cell migration inhibitors by chemical synthesis. *J Am Chem Soc* 126(36):11326–11337
20. Han S, Huang J, Liu B, Xing B, Bordeleau F, Reinhart-King CA et al (2016) Improving fascin inhibitors to block tumor cell migration and metastasis. *Mol Oncol* 10(7):966–980
21. Morris GM, Huey R, Lindstrom W, Sanner MF, Belew RK, Goodsell DS, Olson AJ (2009) AutoDock4 and AutoDockTools4: automated docking with selective receptor flexibility. *J Comput Chem* 30(16):2785–2791
22. Gasteiger J, Marsili M (1980) Iterative partial equalization of orbital electronegativity—a rapid access to atomic charges Y1 - 1980 Y2 - 1980. *Tetrahedron* 36(22):3219–3228 M1 - Generic
23. Huang J, Dey R, Wang Y, Jakoncic J, Kurinov I, Huang XY (2018) Structural insights into the induced-fit inhibition of Fascin by a small-molecule inhibitor. *J Mol Biol* 430(9):1324–1335
24. Sánchez-Linares I, Pérez-Sánchez H, Cecilia JM, García JM (2012) High-throughput parallel blind virtual screening using BINDSURF. *BMC Bioinformatics* 13(Suppl 14):S13
25. Nurmenniemi S, Sinikumpu T, Alahuhta I, Salo S, Sutinen M, Santala M, Risteli J, Nyberg P, Salo T (2009) A novel organotypic model mimics the tumor microenvironment. *Am J Pathol* 175(3):1281–1291
26. Åström P, Heljasvaara R, Nyberg P, Al-Samadi A, Salo T (2018) Human tumor tissue-based 3D in vitro invasion assays. *Methods Mol Biol* 1731:213–221
27. Jelassi B, Chantôme A, Alcaraz-Pérez F, Baroja-Mazo A, Cayuela ML, Pelegrin P, Surprenant A, Roger S (2011) P2X(7) receptor activation enhances SK3 channels- and cystein cathepsin-dependent cancer cells invasiveness. *Oncogene* 30(18):2108–2122
28. Albini A (1998) Tumor and endothelial cell invasion of basement membranes. The matrigel chemoinvasion assay as a tool for dissecting molecular mechanisms. *Pathol Oncol Res* 4(3):230–241
29. Stevenson RP, Veltman D, Machesky LM (2012) Actin-bundling proteins in cancer progression at a glance. *J Cell Sci* 125(Pt 5):1073–1079
30. Esnakula AK, Ricks-Santi L, Kwagyan J, Kanaan YM, DeWitty RL, Wilson LL, Gold B, Frederick WA, Naab TJ (2014) Strong association of fascin expression with triple negative breast cancer and basal-like phenotype in African-American women. *J Clin Pathol* 67(2):153–160
31. García-Solano J, García-Solano ME, Torres-Moreno D, Carbonell P, Trujillo-Santos J, Pérez-Guillermo M, Conesa-Zamora P (2016) Biomarkers for the identification of precursor polyps of colorectal serrated adenocarcinomas. *Cell Oncol (Dordr)* 39(3):243–252
32. Ghebeh H, Al-Khaldi S, Olabi S, Al-Dhfyhan A, Al-Mohanna F, Barnawi R et al (2014) Fascin is involved in the chemotherapeutic resistance of breast cancer cells predominantly via the PI3K/Akt pathway. *Br J Cancer* 111(8):1552–1561
33. Kanda Y, Kawaguchi T, Kuramitsu Y, Kitagawa T, Kobayashi T, Takahashi N, Tazawa H, Habelhah H, Hamada J, Kobayashi M, Hirahata M, Onuma K, Osaki M, Nakamura K, Kitagawa T, Hosokawa M, Okada F (2014) Fascin regulates chronic inflammation-related human colon carcinogenesis by inhibiting cell anoikis. *Proteomics* 14(9):1031–1041
34. Rodríguez-Pinilla SM, Sarrió D, Honrado E, Hardisson D, Calero F, Benitez J, Palacios J (2006) Prognostic significance of basal-like phenotype and fascin expression in node-negative invasive breast carcinomas. *Clin Cancer Res* 12(5):1533–1539
35. Wang CQ, Tang CH, Chang HT, Li XN, Zhao YM, Su CM, Hu GN, Zhang T, Sun XX, Zeng Y, du Z, Wang Y, Huang BF (2016) Fascin-1 as a novel diagnostic marker of triple-negative breast cancer. *Cancer Med* 5(8):1983–1988
36. Salo T, Dourado MR, Sundquist E, Apu EH, Alahuhta I, Tuomainen K, Vasara J, Al-Samadi A (2018) Organotypic three-dimensional assays based on human leiomyoma-derived matrices. *Philos Trans R Soc Lond Ser B Biol Sci* 373(1737):20160482

Publisher's note Springer Nature remains neutral with regard to jurisdictional claims in published maps and institutional affiliations.

Affiliations

Silvia Montoro-García¹  · Begoña Alburquerque-González² · Ángel Bernabé-García³ · Manuel Bernabé-García⁴ · Priscila Campioni Rodrigues^{5,6} · Helena den-Haan⁷ · Irene Luque⁸ · Francisco José Nicolás³ · Horacio Pérez-Sánchez⁹ · María Luisa Cayuela⁴ · Tuula Salo^{5,6,10,11} · Pablo Conesa-Zamora^{2,12} 

¹ Cell Culture Lab. Health Faculty, Universidad Católica de Murcia (UCAM), Campus de los Jerónimos, s/n, Guadalupe, 30107 Murcia, Spain

² Pathology and Histology Department. Health Faculty, Universidad Católica de Murcia (UCAM), Campus de los Jerónimos, s/n, Guadalupe, 30107 Murcia, Spain

³ Molecular Oncology and TGF-β Lab, Biomedical Research Institute of Murcia (IMIB-Arrixaca), Carretera Madrid-Cartagena. El Palmar, Murcia, Spain

⁴ Telomerase, Cancer and Aging Group, University Clinical Hospital “Virgen de la Arrixaca”, Biomedical Research Institute of Murcia (IMIB-Arrixaca) Murcia, Murcia, Spain

⁵ Cancer and Translational Medicine Research Unit, Faculty of Medicine, University of Oulu, Aapistie 5A, FI-90220 Oulu, Finland

⁶ Medical Research Center Oulu, Oulu University Hospital, University of Oulu, Oulu, Finland

⁷ Eurofins Villapharma Research, Parque Tecnológico de Fuente Álamo. Ctra. El Estrecho-Lobosillo, Km 2,5. Av. Azul E, 30320 Murcia, Spain

⁸ Department of Physical Chemistry and Institute of Biotechnology, University of Granada, Campus Fuentenuueva s/n 18071 Granada, Granada, Spain

-
- ⁹ Structural Bioinformatics and High Performance Computing (BIO-HPC) Research Group, Universidad Católica de Murcia (UCAM), Guadalupe, Spain
- ¹⁰ Institute of Oral and Maxillofacial Disease, University of Helsinki, Helsinki, Finland
- ¹¹ HUSLAB, Department of Pathology, Helsinki University Hospital, Helsinki, Finland
- ¹² Clinical Analysis Department, Group of Molecular Pathology and Pharmacogenetics, Biomedical Research Institute from Murcia (IMIB), Hospital Universitario Santa Lucía, c/Mezquita sn, 30202 Cartagena, Spain